Parameter Estimation for Class A Modeled Ocean Ambient Noise

Xuebo Zhang[1],*, Wenwei Ying[2] & Bo Yang[1]

[1]Laboratory of Underwater Acoustics, Middle of Renmin Avenue, Xiashan District, Zhanjiang 524000, China
[2]Naval Research Academy, No. 1 of the Old West Road, Changping District, Beijing 102249, China
*E-mail: xuebo_zhang@sina.cn

Abstract. A Gaussian distribution is used by all traditional underwater acoustic signal processors, thus neglecting the impulsive property of ocean ambient noise in shallow waters. Undoubtedly, signal processors designed with a Gaussian model are sub-optimal in the presence of non-Gaussian noise. To solve this problem, firstly a quantile-quantile (Q-Q) plot of real data was analyzed, which further showed the necessity of investigating a non-Gaussian noise model. A Middleton Class A noise model considering impulsive noise was used to model non-Gaussian noise in shallow waters. After that, parameter estimation for the Class A model was carried out with the characteristic function. Lastly, the effectiveness of the method proposed in this paper was verified by using simulated data and real data.

Keywords: *characteristic function; class A; noise modeling;non-Gaussian noise; parameter estimation; quantile-quantile (Q-Q) plot*.

1 Introduction

The ocean's ambient noise is the main factor limiting the performance of underwater acoustic signal processors. Because of the central limit theorem, most signal processors, such as the communication schemes developed by Istepanian and Stojanovic in [1] and the matched filtering developed by Zhang, *et al*. in [2,3], are based on a Gaussian distribution. Actually, groups of snapping shrimp in warm shallow waters produce an impulsive signal according to Chitre [4]. Besides that, there are also interferences such as industrial noise, strong winds, heavy rain, rainstorms, and so on. These noises display non-Gaussian behavior. Signal processors using a Gaussian noise model are sub-optimal in the presence of non-Gaussian noise. In [5], Jiang, *et al*. have demonstrated that non-linear processors outperform linear processors. In fact, the noise distribution is important for the development of underwater signal processors. With prior knowledge of the noise distribution, optimal or near-optimal signal processors or communication schemes can be designed.

Received March 15th, 2017, 1st Revision June 9th, 2017, 2nd Revision May 9th, 2018, Accepted for publication August 8th, 2018.
 ISSN: 2337-5779, DOI: 10.5614/j.eng.technol.sci.2018.50.3.2

Modeling non-Gaussian noise in water is much slower than in an electromagnetic environment. Traditional noise analysis methods mainly include signal self-correlation, power spectrum estimation, short-time Fourier transform, Wigner-Ville analysis, wavelet analysis, and so on. Second-order statistical characteristics are used by these methods, indirectly adopting a Gaussian model based on Liu's work in [6]. In [7], high-order statistical characteristics including high-order moment and accumulation spectra are employed by Li. Unfortunately, high-order moment and accumulation are usually very complicated, requiring large calculation. Fourth-order moment and accumulation are exploited in practice. Obviously, non-Gaussian noise cannot be completely described. There are many other distributions to model non-Gaussian noise, such as Stein's Gaussian mixture in [8], the Laplacian model developed by Miller and Thomas in [9], and symmetric alpha-stable distribution (SαS) developed by Nikias and Shao in [10]. A Gaussian-Laplacian mixture model cannot truly depict the heavy-tailed characteristic of impulsive noise. The SαS model does not possess finite second-order moment or the closed form of a probability density function. Besides, none of these noise models possess a strong physical or theoretical justification.

In this research, firstly, a quantile-quantile (Q-Q) plot was used to analyze real data. It showed the necessity of investigating a non-Gaussian noise model. Then, ocean ambient noise based on a Class A model was studied. With the characteristic function, the parameters of the Class A model were estimated. Lastly, the processed results of a simulation and real data were used to verify the proposed method.

2 Class A Model

With a complicated formula derivation and some approximations, Middleton deduced the probability density function for Class A noise [11,12]. It can be expressed as:

$$f(x) = \sum_{m=0}^{\infty} \frac{e^{-A} A^m}{m!} \frac{1}{\sqrt{2\pi\sigma_m^2}} \exp\left(-\frac{x^2}{2\sigma_m^2}\right) \tag{1}$$

where m is the number of active impulses. Eq. (1) is a weighted sum of Gaussian distributions. σ_m^2 is the variance of the m-th active impulse. It is given by:

$$\sigma_m^2 = \frac{(\frac{m}{A} + \Gamma)}{1 + \Gamma} \sigma^2 \tag{2}$$

In Eq. (2), $\Gamma \triangleq \delta_G^2 / \delta_I^2$ is the Gaussian to interference noise power ratio with Gaussian noise power δ_G^2 and interference noise power δ_I^2. The total noise power is $\sigma^2 = \delta_G^2 + \delta_I^2$. A is called the impulsive index or overlap index, which describes the intensity with which the impulsive events occur. The noise would tend to be more Gaussian with the increase of A.

In fact, the amplitude distribution of the background noise plays an important role in underwater signal processing or communication schemes. The following parts of this paper will discuss parameter estimation based on the Class A noise model as expressed in Eq. (1).

3 Parameter Estimation Based on Class A Model

3.1 Noise Analyses

The quantile-quantile (Q-Q) plot employed by Zhang, *et al*. in [13] is a graphical method that compares two probability distributions by plotting their quantiles against each other. It is a more powerful approach than the common method of comparing the histograms of samples. To some degree, it is a non-parametric approach to compare the underlying distributions of the samples. Based on the Q-Q plot, the distributions between the collected data and the Gaussian model can be intuitively compared. For N samples $Y = \{y_1, y_2, \cdots, y_N\}$ in ascending order, the quantile function is expressed as:

$$P_i = P\{Y \le q_i\} = \int_{-\infty}^{q_i} \frac{1}{\sqrt{2\pi}} e^{-y^2/2} dy \tag{3}$$

The quantile function specifies the value q_i at which the probability of the random variable Y is less than or equal to the given probability P_i. In Eq. (3), $P_i = (i - 0.5)/N$, $i = 1, 2, \cdots, N$. q_i is the instantaneous amplitude determined by P_i. According to the theory of statistics [13], the relationship between q_i and y_i $(i = 1, 2, \cdots, N)$ is nearly a 45° line when the collected samples are subject to a Gaussian distribution.

Figure 1 shows the real data of the noise. A Q-Q plot of the real data, denoted by the dotted curve, based on the method presented in this section, is shown in Figure 2. A Q-Q plot of the Gaussian data, represented by the dashed line, is also depicted in Figure 2. It is a 45° line. From Figure 2, it can be seen that the middle part of the dotted curve almost follows the 45° line while the tails of the dotted curve deviate from the dashed 45° line. This indicates that the distributions of the real data and the Gaussian data are not identical. If the

Gaussian distribution is used to model the noise, the performance of the underwater signal processors is degraded seriously. Therefore, it is necessary to investigate a non-Gaussian model of ocean ambient noise.

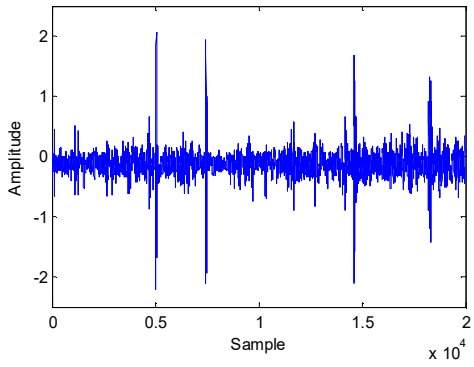

Figure 1 Real data.

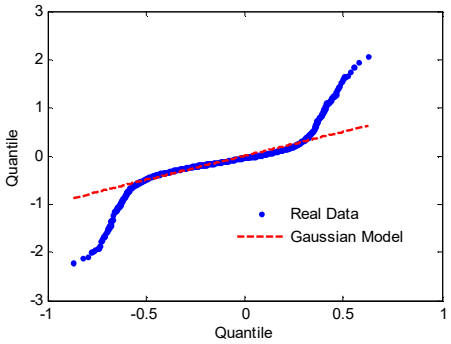

Figure 2 Q-Q plot.

3.2 Characteristic Function of Class A Noise

It is supposed that the random variable Y is subject to a normal Gaussian distribution. The mean value and variance are 0 and σ_G^2, respectively. Based on the definition of the characteristic function from Peebles [14], the characteristic function of Gaussian noise can be easily deduced. The expression is given by:

$$\psi_G(\omega)=\int_{-\infty}^{\infty}\frac{1}{\sqrt{2\pi\sigma_G}}e^{-\frac{y^2}{2\sigma_G^2}}e^{j\omega y}dy=e^{-\frac{\sigma_G^2\omega^2}{2}} \tag{4}$$

where $\omega=\{0,2\pi/M,2\times2\pi/M,\cdots,M\times2\pi/M\}$ is the frequency and M is the number of frequency samples. From Eq. (1), the noise variance can be easily got. It is given by $\delta^2\triangleq \mathrm{E}\left\{|X|^2\right\}=\sum_{m=0}^{\infty}(e^{-A}A^m/m!)\delta_m^2$, which is the average power of the noise. In order to simplify the deduction of the formula, a new variable $K=A\cdot\Gamma$ is introduced. Thus, Eq. (2) can be changed to:

$$\sigma_m^2=\frac{m+K}{A+K}\sigma^2 \tag{5}$$

According to the work developed by Jiang *et al.* in [5], the characteristic function of Class A noise is expressed as:

$$\psi_A(\boldsymbol{\theta},\omega)=\int_{-\infty}^{\infty}f(x)e^{j\omega x}dx=\int_{-\infty}^{\infty}e^{-A}\sum_{m=0}^{\infty}\frac{A^m}{m!}\frac{1}{\sqrt{2\pi\sigma_m^2}}\exp\left(-\frac{x^2}{2\sigma_m^2}+j\omega x\right)dx \tag{6}$$

In Eq. (6), vector $\boldsymbol{\theta}=[\sigma^2, A, K]^{\mathrm{T}}$ denotes the parameter vector. The superscript T represents the transposition. Based on Eq. (4), Eq. (6) is given by:

$$\psi_A(\boldsymbol{\theta},\omega)=\sum_{m=0}^{\infty}\frac{e^{-A}A^m}{m!}\int_{-\infty}^{\infty}\frac{1}{\sqrt{2\pi\sigma_m^2}}\exp\left(-\frac{x^2}{2\sigma_m^2}+j\omega x\right)dx=\sum_{m=0}^{\infty}\frac{e^{-A}A^m}{m!}\exp\left(-\frac{\sigma_m^2\omega^2}{2}\right) \tag{7}$$

Based on Eq. (5), Eq. (7) is expressed as:

$$\begin{aligned}\psi_A(\boldsymbol{\theta},\omega)&=e^{-A}\sum_{m=0}^{\infty}\frac{A^m}{m!}\exp\left\{-\frac{m+K}{2(A+K)}\sigma^2\omega^2\right\}\\&=e^{-A}\sum_{m=0}^{\infty}\frac{A^m}{m!}\exp\left\{-\frac{m\sigma^2\omega^2}{2(A+K)}\right\}\exp\left\{-\frac{K\sigma^2\omega^2}{2(A+K)}\right\}\end{aligned} \tag{8}$$

A new variable $\beta=A\cdot\exp\left(-\frac{\sigma^2\omega^2}{2(A+K)}\right)$ is defined. Thus, Eq. (8) is written as:

$$\begin{aligned}\psi_A(\boldsymbol{\theta},\omega)&=\exp\left\{-\frac{K\sigma^2\omega^2}{2(A+K)}-A\right\}\sum_{m=0}^{\infty}\frac{\beta^m}{m!}\exp(\beta)\exp(-\beta)\\&=\exp\left\{-\frac{K\sigma^2\omega^2}{2(A+K)}-A+\beta\right\}\sum_{m=0}^{\infty}\frac{\beta^m\exp(-\beta)}{m!}=\exp\left\{-\frac{K\sigma^2\omega^2}{2(A+K)}-A+\beta\right\}\end{aligned} \tag{9}$$

Therefore, the characteristic function of Class A noise is given by:

$$\psi_A(\boldsymbol{\theta},\omega)=\exp\left\{-K\frac{\sigma^2\omega^2}{2(A+K)}-A+Ae^{-\frac{\sigma^2\omega^2}{2(A+K)}}\right\} \tag{10}$$

3.3 Parameter Estimation

Based on Eq. (10) and the work developed by Jiang *et al*. in [5], this section mainly concentrates on the algorithm for parameter estimation of the Class A model. The purpose is to estimate the model parameters $\boldsymbol{\theta}=[\Omega, A, K]^{\mathrm{T}}$ with N collected samples. Here, $\Omega=\sigma^2$ is the average power of Class A noise. Based on the natural logarithm, Eq. (10) can be expressed as:

$$\ln\psi_A(\boldsymbol{\theta},\omega)=-K\frac{\Omega\omega^2}{2(A+K)}-A+Ae^{-\frac{\Omega\omega^2}{2(A+K)}} \tag{11}$$

The characteristic function plays an important role in the parameter estimation of the Class A noise model. First, the characteristic function is estimated based on the collected samples. The collected data are divided into L sub-blocks. Each sub-block has N_L samples. The total number of samples is $N=L\cdot N_L$. The characteristic function is estimated through the average operation related to the

characteristic functions of each sub-block. For the *l*-th sub-block, the characteristic function is given by:

$$\hat{\psi}_l(\omega) = \frac{1}{N_L}\sum_{i=1}^{N_L}\exp\{j\omega x_i\} \tag{12}$$

Averaging the characteristic functions related to each sub-block, we get the characteristic function of the collected data. It is expressed as follows:

$$\hat{\psi}(\omega) = \frac{1}{L}\sum_{l=1}^{L}\hat{\psi}_l(\omega) \tag{13}$$

The error, defined as the difference between Eq. (11) and Eq. (13), is given by:

$$\mathbf{F}(\boldsymbol{\theta}) = \ln\psi_A(\boldsymbol{\theta},\omega) - \ln\hat{\psi}(\omega) \tag{14}$$

The parameters $\boldsymbol{\theta} = [\Omega, A, K]^{\mathrm{T}}$ are estimated by minimizing the square error, $\mathbf{F}^{\mathrm{T}}(\boldsymbol{\theta})\mathbf{F}(\boldsymbol{\theta})$. Substituting Eq. (11) into Eq. (14), we get:

$$\mathbf{F}(\boldsymbol{\theta}) = \begin{bmatrix} -K\dfrac{\Omega\omega_0^2}{2(A+K)} - A + Ae^{-\frac{\Omega\omega_0^2}{2(A+K)}} - \ln\hat{\psi}(\omega_0) \\ -K\dfrac{\Omega\omega_1^2}{2(A+K)} - A + Ae^{-\frac{\Omega\omega_1^2}{2(A+K)}} - \ln\hat{\psi}(\omega_1) \\ \vdots \\ -K\dfrac{\Omega\omega_M^2}{2(A+K)} - A + Ae^{-\frac{\Omega\omega_M^2}{2(A+K)}} - \ln\hat{\psi}(\omega_M) \end{bmatrix}_{M\times 1} \tag{15}$$

Based on the method of steepest descent, the gradient of the square error $\mathbf{F}^{\mathrm{T}}(\boldsymbol{\theta})\mathbf{F}(\boldsymbol{\theta})$ is expressed as $\mathbf{D}^{\mathrm{T}}(\boldsymbol{\theta})\mathbf{F}(\boldsymbol{\theta})$. The error derivation $\mathbf{D}(\boldsymbol{\theta})$ is:

$$\mathbf{D}(\boldsymbol{\theta}) = \frac{\partial\mathbf{F}(\boldsymbol{\theta})}{\partial\boldsymbol{\theta}^{\mathrm{T}}} = \begin{bmatrix} D_\Omega(\omega_0) & D_A(\omega_0) & D_K(\omega_0) \\ D_\Omega(\omega_1) & D_A(\omega_1) & D_K(\omega_1) \\ \vdots & \vdots & \vdots \\ D_\Omega(\omega_M) & D_A(\omega_M) & D_K(\omega_M) \end{bmatrix}_{M\times 3} \tag{16}$$

According to Eq. (15), the elements in Eq. (16) are given by:

$$
\begin{aligned}
D_{\Omega}(\omega_k) &= -\frac{K\omega_k^2}{2(A+K)} - \frac{A\omega_k^2}{2(A+K)} e^{-\frac{\Omega\omega_k^2}{2(A+K)}} \\
D_{A}(\omega_k) &= \frac{\Omega K\omega_k^2}{2(A+K)^2} - 1 + \left[1 + \frac{A\Omega\omega_k^2}{2(A+K)^2}\right] e^{-\frac{\Omega\omega_k^2}{2(A+K)}} \\
D_{K}(\omega_k) &= -\frac{\Omega\omega_k^2}{2(A+K)} + \frac{\Omega K\omega_k^2}{2(A+K)^2} + \frac{A\Omega\omega_k^2}{2(A+K)^2} e^{-\frac{\Omega\omega_k^2}{2(A+K)}}
\end{aligned} \tag{17}
$$

Using the gradient of the square error, the adjustment quantity is expressed as:

$$
\Delta\boldsymbol{\theta}^r = -\left[\mathbf{D}^{\mathrm{T}}(\boldsymbol{\theta}^r)\mathbf{D}(\boldsymbol{\theta}^r) + \delta\mathbf{I}\right]^{-1}\mathbf{D}^{\mathrm{T}}(\boldsymbol{\theta}^r)\mathbf{F}(\boldsymbol{\theta}^r) \tag{18}
$$

In Eq. (18), the gradient is further normalized by $\mathbf{D}^{\mathrm{T}}(\boldsymbol{\theta}^r)\mathbf{D}(\boldsymbol{\theta}^r)$. $\delta\mathbf{I}$ is used to overcome the numerical instability of $\mathbf{D}^{\mathrm{T}}(\boldsymbol{\theta}^r)\mathbf{D}(\boldsymbol{\theta}^r)$. δ is a regularization parameter; and $\mathbf{I}$ is the unit matrix. The superscript r represents the r-th iteration. Then, the parameters are updated based on the adjustment quantity as shown in Eq. (18). The updated parameters used in the next iteration are given by:

$$
\boldsymbol{\theta}^{r+1} = \boldsymbol{\theta}^r + \mu\Delta\boldsymbol{\theta}^r \tag{19}
$$

In Eq. (19), μ is the step factor. A block diagram of the proposed method based on the method of steepest descent is shown in Figure 3. First, the parameters $\boldsymbol{\theta} = [\Omega, A, K]^{\mathrm{T}}$ are initialized. Based on Eqs. (15) and (16), the error and derivation are calculated in the second step. In the third step, the adjustment quantity of the parameters is calculated with Eq. (18). Then, the parameters are updated using Eq. (19). The iteration stops when square error $\mathbf{F}^{\mathrm{T}}(\boldsymbol{\theta})\mathbf{F}(\boldsymbol{\theta})$ is constrained within the expected error. Otherwise, the iteration continues with the second step in Figure 3.

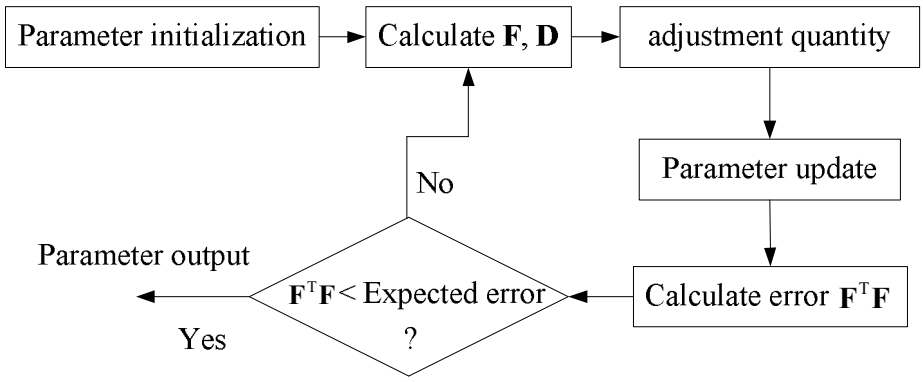

Figure 3 Block diagram of the proposed method.

4 Data Processing Results

4.1 Simulation Experiment

Simulated data were used to test the proposed method. The parameters used for the Class A noise simulation were $A = 0.15$, $\Gamma = 0.002$, and $\Omega = 2.5$. With the proposed method, the estimated results of the impulsive index, the product between the impulsive index and the Gaussian to interference noise power ratio (PIR), and the noise power are shown in Figures 4, 5, and 6, respectively. From these figures, it can be seen that the proposed method possesses the highest convergence speed. After 50 iterations, the estimated parameters were tending towards stability. Besides, the estimated parameters are close to the theoretical values. This means that the proposed method can accurately estimate the parameters for the Class A noise model.

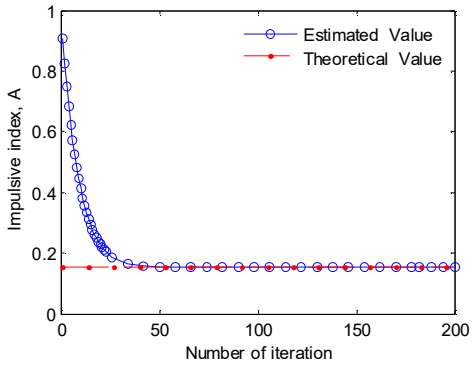

Figure 4 Impulsive index of simulated data.

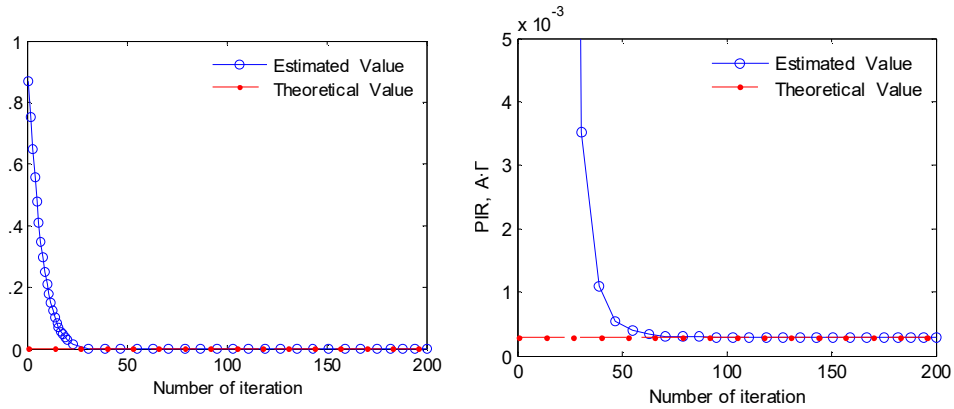

(a) (b)

Figure 5 Product of impulsive index and the Gaussian to interference noise power ratio (PIR). (a) PIR of simulated data; (b) closer look.

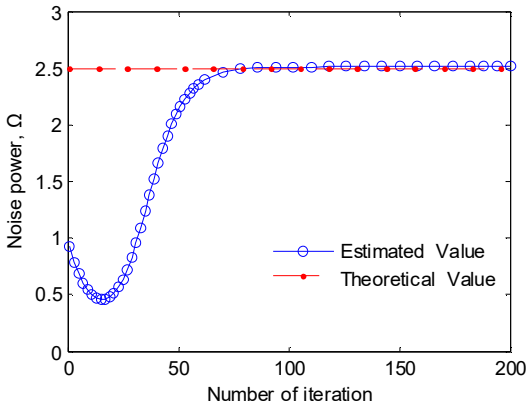

Figure 6 Noise power of simulated data.

Based on the simulated data, the empirical characteristic function can be obtained with Eqs. (12) and (13). With the simulation parameters for the Class A noise model, the theoretical characteristic function can be calculated. Using the estimated parameters, the estimated characteristic function is got. Therefore, three characteristic functions are obtained for the simulated noise. Comparing the estimated characteristic function with the empirical data and the theoretical data, the performance of the proposed method can be easily found. Figure 7 shows the three characteristic functions described above. From Figure 7, the estimated characteristic function agrees well with the empirical and the theoretical data, which further verifies the effectiveness of the method proposed in this paper.

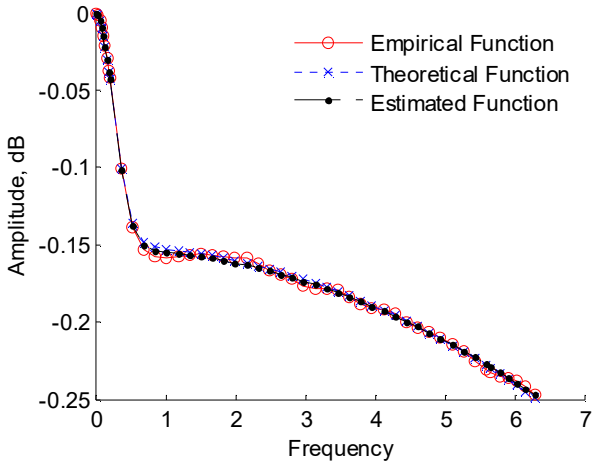

Figure 7 Characteristic function of simulated data.

The amplitude probability distribution (APD) used by Field and Lewinstein in [15] and by Chrissan in [16] describes the statistical property of random signals. It is defined as the cumulative distribution of the probability that noise amplitude x exceeds a specified threshold, x_0. It is written as:

$$APD(x_0) = P(|x| > x_0) \tag{20}$$

The horizontal axis of APD denotes the probability $P(|x| > x_0)$, while the threshold x_0 is represented by the vertical axis. In practice, both axes are adjusted by the lognormal operations $-0.5\lg\left(-\ln P(|x| > x_0)\right)$ and $10\log_{10}(x_0)$, respectively. After the lognormal operations, the APD of the Gaussian noise is transformed to a straight line.

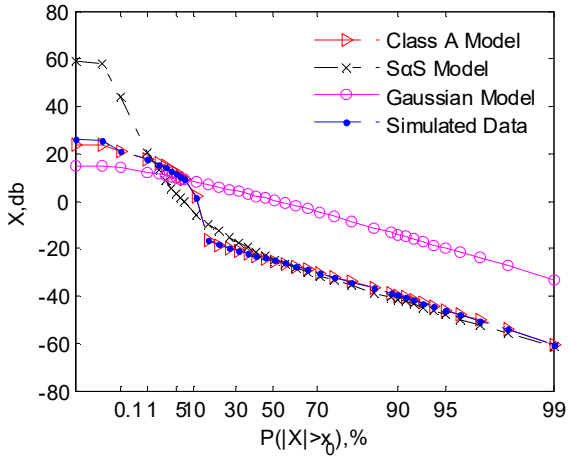

Figure 8 APD of simulated data.

It is well known that Gaussian distribution is uniquely determined by two parameters, i.e. the mean value and the variance. With the mean value and the variance of the simulated data, the APD of Gaussian noise can be depicted as shown in Figure 8. It is a straight line, which cannot describe the simulated data due to their non-Gaussian properties. Based on the log method used by Nikias and Shao in [10], the parameters of the SαS model, i.e. the characteristic exponent and the scale parameter, can be estimated. Then, the APD of the noise in the SαS model is obtained. Observing the APD of the SαS model in Figure 8, the lower portion of the curve is in very good agreement with the curve of the simulated data. However, the upper portion of the curve is far removed from the curve of the simulated data. This indicates that the SαS model cannot describe impulsive noise. Using the method proposed in this paper, we can get the estimated parameters of the Class A model. Then, the APD is plotted, as shown

in Figure 8. It can be seen that the curve of the Class A model agrees well with the curve of the simulated data. This means that the Class A model can describe the simulated data well.

4.2 Real Data Processing

This section deals with the real data shown in Figure 1. The estimated results of the impulsive index, PIR, and the signal power are shown in Figures 9, 10, and 11, respectively. Observing these figures, the same conclusions can be drawn as described in Section 4.1. With the real data, the estimated parameters tend towards stability after 40 iterations. Meanwhile, the estimated noise power represented by the solid curve in Figure 11 is close to the statistical power indicated by the dashed line.

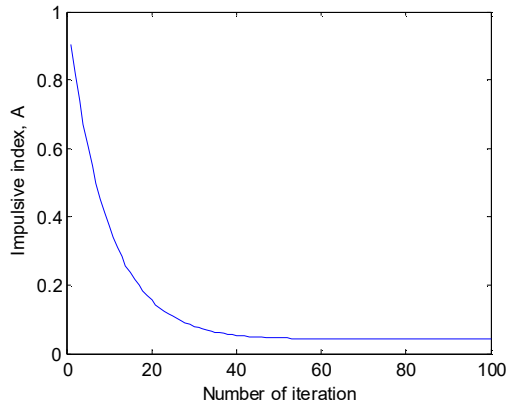

Figure 9 Impulsive index of the real data.

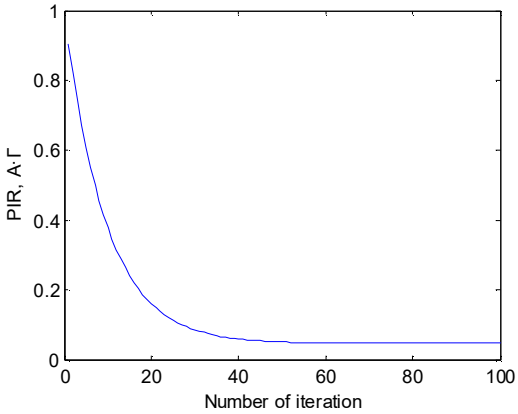

Figure 10 Product of impulsive index and the Gaussian to interference noise power ratio (PIR).

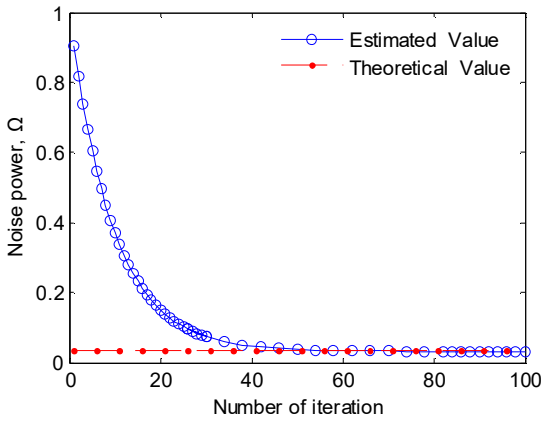

Figure 11 Noise power of the real data.

Figure 12 shows the empirical characteristic function, the characteristic function after the first iteration and the characteristic function after the last iteration. Compared with the empirical characteristic function, the characteristic function after the first iteration does not meet the requirements of parameter estimation. However, the characteristic function after the last iteration agrees almost completely with the empirical one. This indicates that the presented method is effective for parameter estimation of the Class A model. Figure 13 shows the APDs related to the Class A model, the SαS model, the Gaussian model, and the real data. From this figure, the same conclusions can be drawn as in the previous section.

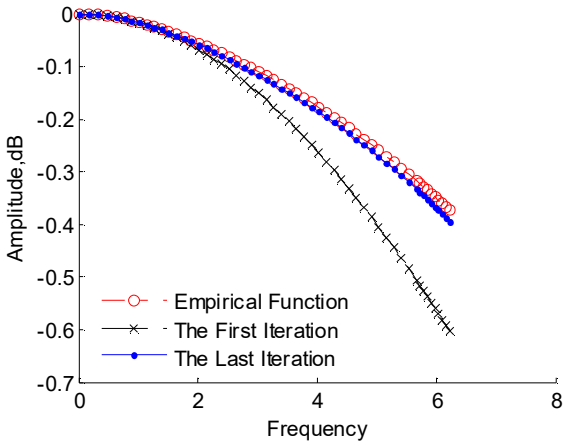

Figure 12 Characteristic function of the real data.

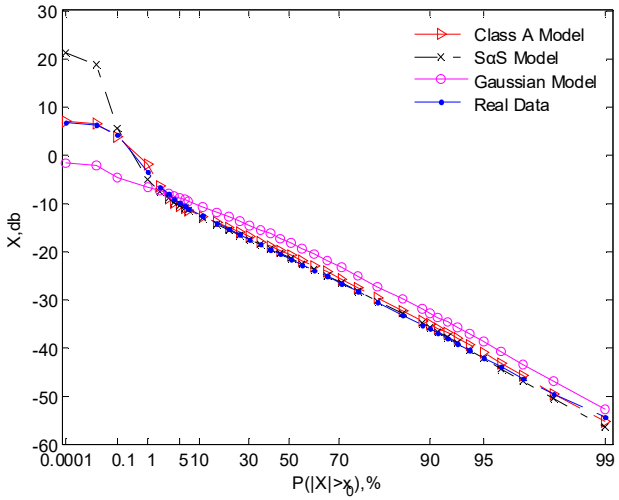

Figure 13 APD of the real data.

Based on the simulation experiment and the real data processing results, the impulsive noise cannot be simply modeled with traditional noise models, because it would degrade the performances of subsequent signal processors, such as signal detection, communication, and so on.

5 Conclusions

In shallow waters there are high deviations in the amplitude of the noise samples due to impulsive noise. The distribution of this noise decays slower in the tails than the Gaussian model predicts. If signal processors developed in a Gaussian noise channel are used, their performance degrades. Thus, the Gaussian distribution is not suitable for modeling impulsive noise. Based on the Q-Q plot, it was shown that real data from shallow waters are not subject to the Gaussian model. Actually, the distribution of ocean ambient noise plays an important role in the development of underwater acoustic signal processors. In this study, the most famous heavy-tailed distribution, i.e. the Middleton Class A model, was used to describe impulsive noise in shallow waters. Along with the characteristic function, a parameter estimation method was presented. The processing results of simulated and real data showed that the proposed method has a high convergence speed. Besides, the estimated parameters were close to the theoretical values. Therefore, the conclusion can be drawn that the Class A model can effectively describe impulsive noise in shallow waters.

Acknowledgements

This work was supported by the National Nature Science Foundation in China under grant no. 61601473 and the National Key Laboratory Foundation in China under grant no. 9140C290401150C29132.

Nomenclature

A	=	impulsive index or overlap index
$\mathbf{D}$	=	error derivation
$\mathbf{F}$	=	error between characteristic function of empirical data and that of real data
f	=	probability density function
K	=	product between impulsive index and Gaussian to interference noise power ratio
L	=	total number of segmented sub-blocks
m	=	number of active impulses
M	=	the number of frequency samples
N	=	total samples of collected data
N_L	=	number of sampled data for the l-th block
P	=	probability
Γ	=	Gaussian to interference noise power ratio
δ	=	regularization parameter
$\boldsymbol{\theta}$	=	parameter vector
$\Delta\boldsymbol{\theta}$	=	corrective value of parameters
μ	=	step size
σ^2	=	noise power
δ_G^2	=	Gaussian noise power
δ_I^2	=	interference noise power
σ_m^2	=	power of the m-th active impulse
$\hat{\psi}$	=	statistical characteristic function with collected data
ψ_A	=	characteristic function of Class A noise
ψ_G	=	characteristic function of Gaussian noise
$\hat{\psi}_l$	=	statistical characteristic function for the l-th block
ω	=	frequency
Ω	=	noise power

References

[1] Istepanian, R. & Stojanovic, M., *Underwater Acoustic Digital Signal Processing and Communication Systems*, ed. 1, Kluwer Academic Publishers, USA, 2002.

[2] Zhang, X.B., Tang, J.S. & Zhong, H.P., *Multireceiver Correction for the Chirp Scaling Algorithm in Synthetic Aperture Sonar*, IEEE Journal of Oceanic Engineering, **39**(3), pp. 472-481, Jul. 2014.

[3] Zhang, X.B., Huang, H.N., Ying, W.W., Wang, H.K. & Xiao, J., *An Indirect Range-Doppler Algorithm for Multireceiver Synthetic Aperture Sonar Based on Lagrange Inversion Theorem*, IEEE Transactions on Geoscience and Remote Sensing, **55**(6), pp. 3572-3587, Jun. 2017.

[4] Chitre, M., *Underwater Acoustic Communications in Warm Shallow waters Channels*, Ph. D Dissertation, Electrical & Computer Engineering, National University of Singapore, Singapore, 2006.

[5] Jiang, Y.Z., Ying, W.W, Zhang, S.X., Guo, G.H. & Li, C.J., *Non-Gaussian Noise Model of Extremely Low Frequency Channel and Its Application,* National Defense Industry Press, China, 2014.

[6] Liu, Z.Q., *Signal Detection in Non-Gaussian Reverberation Background*, Master dissertation, College of Underwater Acoustic Engineering, Harbin Engineering University, Harbin, China, Mar. 2008.

[7] Li, C.P., *Research on the Identification Method of Non-Gaussian ARMA Model Based on High-order Statistics*, Master dissertation, National University of Defense Technology, Changsha, China, Jan. 2002.

[8] Stein, D., *Detection of Random Signals in Gaussian Mixture Noise,* IEEE Trans. Inf. Theory, **41**(6), pp. 1788-1801, Nov. 1995.

[9] Miller, J.H. & Thomas, J.B., *The Detection of Signals in Impulsive Noise Modeled as a Mixture Process*, IEEE Trans. Commu., **COM-24**(5), pp. 559-563, May 1976.

[10] Nikias, C.L. & Shao, M., *Signal Processing with Alpha-stable Distribution and Application,* John Wiley & Sons, Inc., USA, 1995.

[11] Middleton, D., *Statistical-physical Models of Urban Radio-noise Environments-part I: Foundations*, IEEE Transactions on Electromagnetic Compatibility, **EMC-14**(2), pp. 38-56, May 1972.

[12] Middleton, D., *Procedures for Determining the Parameters of the First-order Canonical Models of Class A and Classs B Electromagnetic Interference*, IEEE Transactions on Electromagnetic Compatibility, **EMC-21**(3), pp. 190-208, Aug. 1979.

[13] Zhang, S.X., Xu, D. Y., Jiang, Y.Z. & Bi, W.B., *Probability Model Identification for Amplitude of Extremely Low Frequency Atmospheric Noise*, Journal of Applied Sciences Electronics and Information Engineering, **26**(4), pp. 336-341, Jul. 2008.

[14] Peebles Jr., P.Z., *Probability Random Variables and Random Signal Principles*, McGraw-Hill, USA, 1980.
[15] Field, E. & Lewinstein, M., *Amplitude-probability Distribution Model for VLF/ELF Atmospheric Noise*, IEEE Transactions on Communications, **26**(1), pp. 83-87, Jun. 1978.
[16] Chrissan, D.A., *Statistical Analysis and Modeling of Low-frequency Radio Noise and Improvement of Low-frequency Communications*, PhD dissertation, Stanford University, USA, 1998.